Self-organized stiffness in regular fractal polymer structures

Marco Werner and Jens-Uwe Sommer
Leibniz-Institut für Polymerforschung Dresden e.V., Hohe Strasse 6, 01069 Dresden, Germany and
Technische Universität Dresden, Institute of Theoretical Physics, 01069 Dresden, Germany
(Received 28 January 2011; published 16 May 2011)

We investigated membrane-like polymer structures of fractal connectivity such as Sierpinski gaskets and Sierpinski carpets applying the bond fluctuation model in three dimensions. Without excluded volume (phantom), both polymeric fractals obey Gaussian elasticity on larger scales determined by their spectral dimension. On the other hand, the swelling effect due to excluded volume is rather distinct between the two polymeric fractals: Self-avoiding Sierpinski gaskets can be described using a Flory-type mean-field argument. Sierpinski carpets having a spectral dimension closer to perfect membranes are significantly more strongly swollen than predicted. Based on our simulation results it cannot be excluded that Sierpinski carpets in athermal solvent show a flat phase on larger scales. We tested the self-consistency of Flory predictions using a virial expansion to higher orders. From this we conclude that the third virial coefficient contributes marginally to Sierpinski gaskets, but higher order virial coefficients are relevant for Sierpinski carpets.

DOI: 10.1103/PhysRevE.83.051802 PACS number(s): 36.20.Ey, 61.25.hp, 61.43.−j

I. INTRODUCTION

Polymerized or tethered membranes can be obtained experimentally by polymerization of functional groups grafted to a lipid bilayer [1,2] or in the form of graphite oxide sheets [3]. The striking characteristics of tethered membranes have attracted much interest during the past decades. One intriguing aspect is the flat (stretched) state which they show in good solvent. The linear relation $R \propto L^{\nu}$ with $\nu = 1$ between radius of gyration and linear extension of the membrane has been pointed out by computer simulations [4–9]. One may wonder why a long-range order between surface normals is entropically favored over crumpled structures. Actually there are several arguments which help to understand this phenomenon [10].

It has been shown that excluded volume acts on local scales as an effective bending rigidity because of the exclusion of large bending angles [11]. It is also known that local bending rigidities amplify on increasing scales due to fluctuations on the tethered backbone which reduce Gaussian curvatures [12–14]. Thus, a locally induced bending rigidity may exceed a critical value resulting in a transition from crumpled to stretched equilibrium states [15–17]. It has been proven that even marginal excluded volume interactions override the crumpling transition and tethered membranes are universally flat [8]. The usual concepts of polymer physics such as the Flory argument [18–20] and ϵ expansions [21,22] are not able to predict the membranes' flatness. This stands in marked contrast to polymer chains where ϵ expansions yield good estimates and the Flory prediction overestimates the swelling effect slightly [23]. The quality of the Flory prediction can thus be seen as an indicator of the presence of self-organized bending stiffness.

We are interested in the correlation between the connectivity of a structure and the appearance of self-organized stiffness. How does the deviation between Flory theory and real structures evolve with chemical dimension in the interval $1 < D < 2$, that is, between chainlike structures and perfect membranes? Here, networks with fractal connectivity are interesting model systems for analyzing the quality of Flory prediction depending on connectivity. Off-lattice Monte Carlo simulations of Sierpinski gaskets [24] have been carried out in three dimensions and show a crumpled structure in accordance with the Flory prediction. This indicates that stiffening on larger scales due to local excluded volume is much weaker than in tethered membranes. Furthermore, simulations in embedding spaces $3 \leqslant d \leqslant 14$ give an estimate for the upper critical dimension of Sierpinski gaskets (SGs) which is also consistent with the Flory model [24]. Monte Carlo simulations of SGs in two embedding space dimensions [25] show that the Flory prediction, $\nu_F = 0.977$, slightly underestimates the simulation result $\nu = 1.002 \pm 0.005$. It has been concluded that in $d = 2$ polymeric SGs are asymptotically stretched with $R \propto L$. It was also shown that the elasticity of SGs in $d = 2$ is dominated by excluded volume interactions which stabilize the structure instead of entropic forces [25,26].

Since SGs in three embedding dimensions [24] are crumpled, one may expect either a smooth crossover or a sudden appearance of a stretched structure when tuning the chemical dimension from that of SGs to that of membranes. We use the bond fluctuation model to simulate polymeric Sierpinski gaskets as well as Sierpinski carpets, where the latter ones probe a chemical dimension within this interval. We will show throughout this paper that Sierpinski carpets (SCs) without excluded volume are crumpled according to Gaussian elasticity. On the other hand, our simulations of self-avoiding SCs show a significantly stronger swelling effect than predicted by the Flory model. Using a self-consistency analysis of the Flory argument for SCs in good solvents we find that higher order virial terms can essentially contribute to conformation statistics. This might explain the appearance of quasiflat conformations and large deviations from Flory predictions.

The rest of this paper is organized as follows. In Sec. II we summarize the Flory model for polymeric fractals. In Sec. III we present the Monte Carlo method we have used to simulate those structures on a lattice. Section IV discusses simulation results which are compared to the predictions of Sec. II. Our conclusions are given in Sec. V.

II. STATIC PROPERTIES OF POLYMERIC FRACTALS

The linear size L of a network is given by the number of chemical units forming the shortest path between characteristic bounding monomers. The mass N of a polymeric fractal with self-similar connectivity is a power of L,

$$N \propto L^D, \tag{1}$$

where we call D the *chemical* dimension. A network of self-similar connectivity which is driven locally by Brownian kicks will form a self-similar structure in the embedding space. The relation between the radius of gyration, R, and the mass of a self-similar structure defines the Hausdorff dimension d^H:

$$R \propto N^{1/d^H} \propto L^{\nu} \quad \text{with} \quad \nu\, d^H = D. \tag{2}$$

First, consider a phantom polymeric fractal without self-avoidance and with harmonic bond potentials. The typical spatial extension R_0 of such a Gaussian network can be calculated regarding the eigenvalues of a generalized Rouse matrix which is a discretized representation of the Laplacian $-\Delta$ on the network. Considering the spectral density at small eigenvalues one can show [18,27,28] that

$$\left\langle R_0^2 \right\rangle \propto N^{2/d_s - 1}. \tag{3}$$

Here the spectral dimension d_s is an intrinsic network parameter characterizing various static and dynamic properties [29] that depend on connectivity only. Consider, for instance, a random walker on a fractal network. It was shown that the mean number of distinct nodes visited during the time t is given by [30,31]

$$S_w \propto t^{d_s/2}. \tag{4}$$

Regarding Eq. (3), it is worth mentioning that the Hausdorff dimension of a Gaussian network,

$$d_0^H = \frac{2d_s}{2 - d_s}, \tag{5}$$

does not depend on any other dimension than d_s. The spatial appearance of a Gaussian network in embedding spaces is determined by connectivity only. Vice versa, the spectral dimension of a Gaussian network can be calculated using its Hausdorff dimension d_0^H in arbitrary space dimension $\geqslant 1$.

To estimate the swelling behavior of a network in the presence of excluded volume, one can choose a mean-field ansatz for the free-energy difference δF between Gaussian and swollen networks [18] following the Flory idea:

$$\frac{\delta F}{kT} \propto \frac{\nu N^2}{R^d} + \frac{3R^2}{2R_0^2}. \tag{6}$$

Here, R is the unknown size of the swollen network in a d-dimensional embedding space, and ν is the excluded volume parameter. The first term of Eq. (6) describes a penalty for pair contacts assuming a homogeneous monomer density in a sphere of volume R^d. The second term represents the stretching energy of a Gaussian spring with mean radius of gyration R_0, see Eq. (3). Minimization of δF with respect to R yields the Flory estimates [18],

$$d_F^H = \frac{d_s(d+2)}{d_s+2}, \quad \nu_F = \frac{D(d_s+2)}{d_s(d+2)}. \tag{7}$$

Note that d_F^H is experimentally accessible in scattering experiments. Although Eq. (6) neglects density fluctuations and overestimates both contributions [32], prediction (7) yields reasonable exponents, for instance, for polymer chains and Sierpinski gaskets in three space dimensions.

In order to calculate the spectral dimension based on Eq. (5) the polymeric fractal (without excluded volume constraints) must display Gaussian elasticity on the relevant length scales. It is well accepted that ideal chains ($d_s = 1$) belong to the universality class of Gaussian elasticity. For tethered membranes ($d_s = 2$), on the other hand, there are indications for a Gaussian fixed point [20]: Applying the Migdal-Kadanoff renormalization [33] it was shown that various isotropic bond potentials can be replaced by effective harmonic springs on larger scales [20]. Various simulation results [9,19,34] confirm these indications, as they reproduce the logarithmic behavior $R^2 \propto \ln(L)$ corresponding to $d_0^H = \text{“}\infty\text{”}$ as predicted by Eq. (5). For phantom membranes with fractal connectivity in between chains and membranes ($1 < d_s < 2$) previous simulation studies have considered this problem. In particular, phantom Sierpinski gaskets have been studied in $d = 2$ [25] as well as in $d = 3$ and $d = 9$ space dimensions [24] using Monte Carlo simulations with box potentials for the bonds. Their Hausdorff dimension is consistent with prediction (5) using the theoretical spectral dimension of Sierpinski gaskets.

In the following we implement polymeric Sierpinski gaskets as well as Sierpinski carpets within a 3-dimensional lattice Monte Carlo model. We obtain estimates for the spectral dimensions d_s of both fractals using the Hausdorff dimensions in the phantom case and Eq. (5), where we assume Gaussian elasticity. As will be shown, our results for d_s are consistent with previous theoretical and numerical predictions, which justifies the latter assumption a posteriori. In a next step, we compare the Flory prediction (7) based on the obtained d_s to simulation results for self-avoiding networks.

III. MONTE CARLO SIMULATIONS

We used the bond fluctuation model (BFM) [35,36] which is a dynamical Monte Carlo method. This model features a high abstraction level for studying the universal dynamic and static properties of polymer structures efficiently [37–40]. Monomers are formed by cubes occupying eight neighboring sites on a simple cubic unit lattice. The cubes are not allowed to overlap which implements excluded volume. A chemical bond between two monomers is implemented as the constraint of their distance to a set of 108 vectors with maximum length $\sqrt{10}$. An elementary simulation step consists of the random selection of one monomer as well as one of six possible jump vectors to neighboring sites. The selected monomer is displaced by this vector, if excluded volume and bond requirements are fulfilled. One can show that bonds will never cross each other within one elementary step [35,41]; thus local topology is conserved. A time unit “Monte Carlo Step” (MCS) is defined as the average number of attempted moves per monomer. The model can also be used to simulate phantom structures by switching off all excluded volume constraints.

The BFM was used to simulate polymer structures with the connectivity of regular fractals focusing on Sierpinski gaskets and Sierpinski carpets, see Figs. 1(a) and 1(b). Structures with

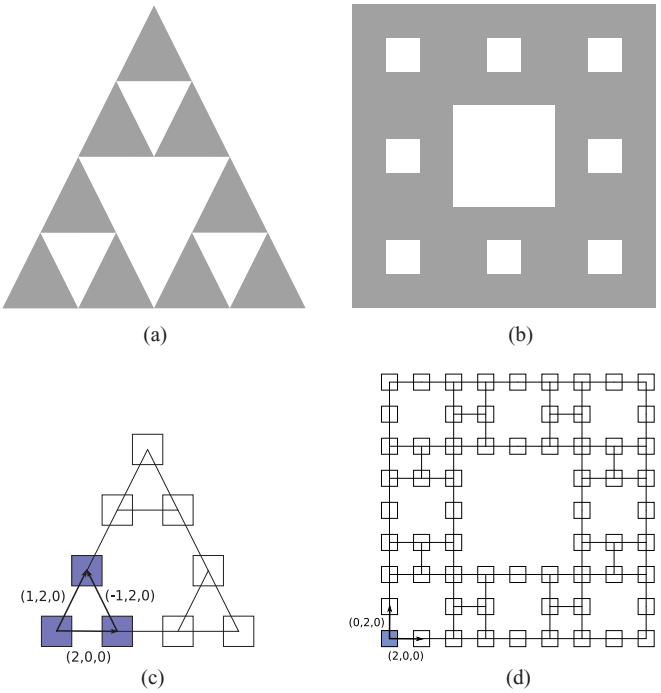

FIG. 1. (Color online) Mass distributions of Sierpinski gaskets (a) and Sierpinski carpets (b) of generation $g = 2$ compared to corresponding connectivities, which were used for simulations with the BFM. The connectivity of a Sierpinski gasket in the BFM is shown in (c), where the filled squares sketch a triangle of $g = 1$. Part (d) shows a Sierpinski carpet in the BFM. The filled square sketches a carpet of $g = 0$.

excluded volume as well as phantom structures have been simulated. The chemical dimensions $D_\triangle$ of the Sierpinski gaskets and $D_\square$ of Sierpinski carpets are [42]

$$D_\triangle = \frac{\ln(3)}{\ln(2)} = 1.585, \quad D_\square = \frac{\ln(8)}{\ln(3)} = 1.893. \tag{8}$$

One may create approximative representations of a regular fractal by iterative arrangement of rescaled self-copies g times, where g is called the generation. Generally, mapping regular fractals to computing systems implies limiting the degree of self-similarity due to the limited memory or the corresponding simulation time. As we regard polymer structures, we have

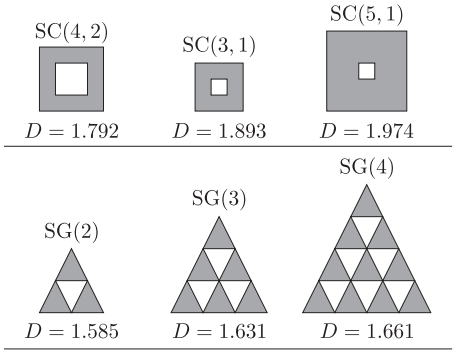

FIG. 2. Selection of various two-dimensional generators according to the classes of Sierpinski carpets, SC(b,l), and generalized Sierpinski gaskets, SG(b), where the rescaling of linear size is given by b and the linear size of the inner cut of SC generators is given by l.

to introduce discrete monomers and connectivities on local scales. Thus Figs. 1(c) and 1(d) in fact show *dual* versions of SGs and SCs, respectively. Our simulation setups and relaxation times are summarized in Table I. We note that simulations of phantom SCs of generation $g = 6$ were carried out using a parallel version of the BFM which was programmed for graphical processing units and run on an "NVIDIA GeForce GTX 480" for about three weeks. Details of this method will be published elsewhere.

SGs and SCs as shown in Fig. 1 can be associated with more general classes of regular fractals. Figure 2 presents examples of generators of the classes of planar and symmetric SCs and SGs, respectively. In principle, arbitrary generators could be mapped to polymer models such as the BFM. However, in this work we concentrate on connectivities as shown in Fig. 1. Typical simulation snapshots of corresponding self-avoiding structures are shown in Fig. 3.

IV. RESULTS AND DISCUSSION

To analyze the simulated fractal networks we take into account their self-similarity and analyze subnetworks of various linear extensions L. For all networks of different size we calculated the radius of gyration, R, to obtain exponents ν or d^H as best fits with respect to Eq. (2). Simulation results

TABLE I. Overview of simulation setups including system sizes N and simulation times t. The simulation times t do not include the equilibration time of flat initial configurations, where we waited at least of the order of 10^8 MCS before calculating any observable. For the SC of generation $g = 6$ we waited 10^9 MCS. The relaxation times τ_R were obtained using exponential fits of the autocorrelation function of the largest eigenvalue of the gyration tensor. The number of decorrelated states was estimated by $t/2.3\tau_R$, where the autocorrelation approaches 0.1.

			Phantom			Self-Avoiding		
	g	N	t	τ_R	$t/2.3\tau_R$	t	τ_R	$t/2.3\tau_R$
△ SGs	7	2187	5.0×10^8	4.2×10^5	514	9.8×10^9	4.2×10^6	1020
	8	6561	9.1×10^9	2.3×10^6	1723	6.0×10^9	3.2×10^7	82
	9	19683	2.5×10^9	7.6×10^6	140	1.7×10^9	9.5×10^7	8
□ SCs	4	4096	9.2×10^9	1.4×10^5	2.8×10^4	1.7×10^{10}	4.5×10^6	1651
	5	32768	1.0×10^9	1.9×10^6	227	2.0×10^9	1.7×10^7	50
	6	262144	2.4×10^9	1.7×10^7	62			

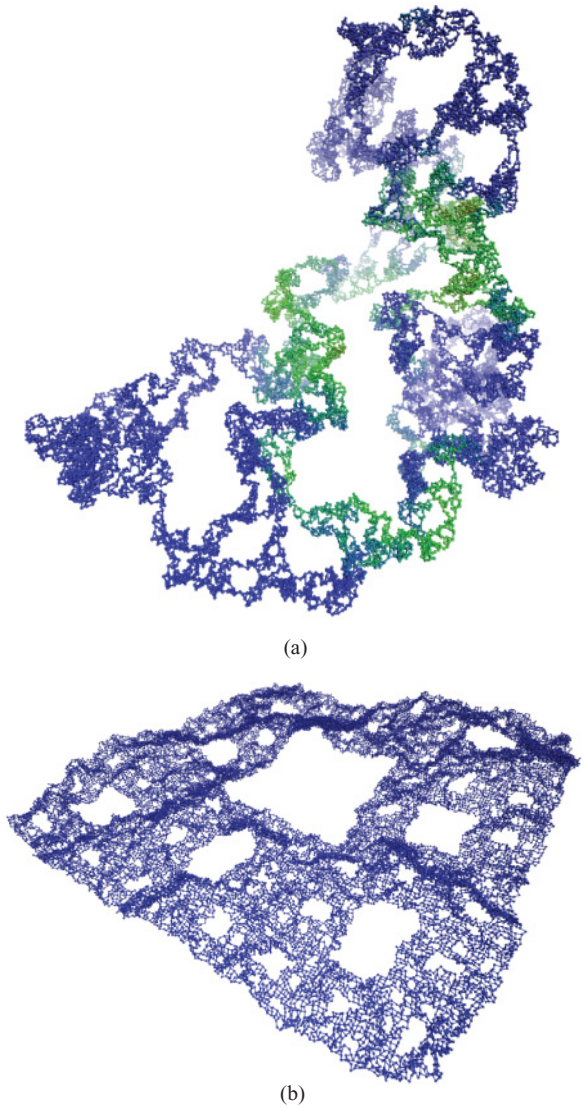

FIG. 3. (Color online) Snapshots of BFM simulations of self-avoiding (a) Sierpinski gasket of generation $g = 8$, and (b) Sierpinski carpet of generation $g = 5$.

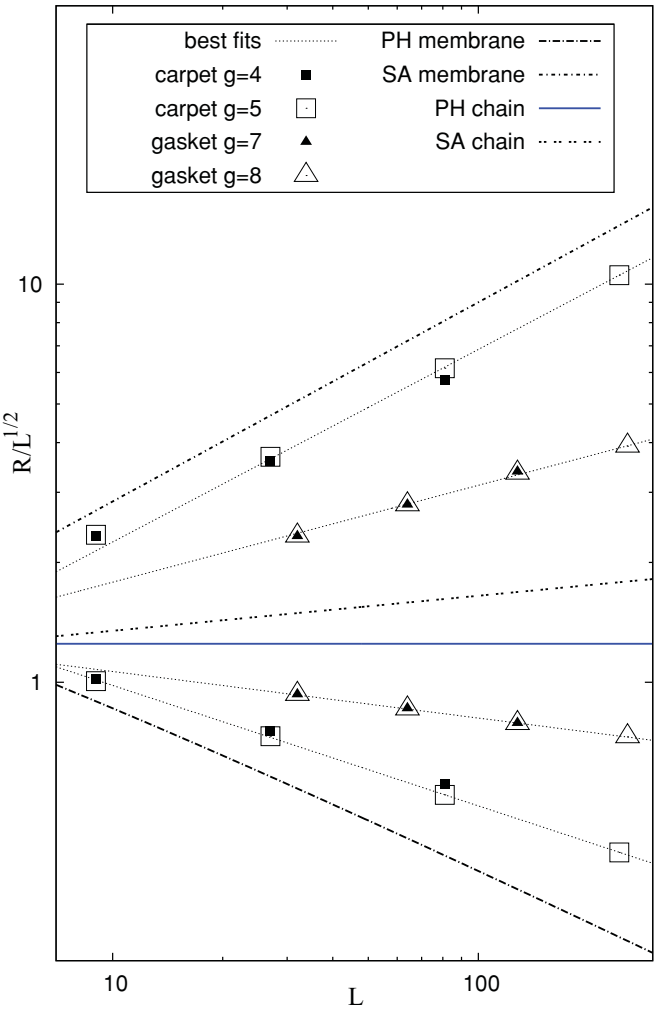

FIG. 4. (Color online) Rescaled radii of gyration, R, as function of the linear size, L, of fractal polymer structures with various connectivities as obtained using the BFM. Simulation results are compared to phantom and self-avoiding membranes and polymer chains by illustrating their slopes using thicker lines. The horizontal line corresponds to ideal chains. Phantom (PH) structures except ideal chains show negative slopes whereas self-avoiding (SA) structures have positive slopes in this representation. The difference between the slopes of phantom and self-avoiding structures increases with chemical dimension. Results for Sierpinski gaskets (triangles) are obtained using the gyration radii of edges of various subtriangles which are multiplied by a factor 1.2 for better discrimination between the data sets. For Sierpinski carpets (squares) we show the radius of gyration of subcarpets depending on the linear size L of their edges.

for $R(L)$ of SGs and SCs are shown in Fig. 4, compared to linear chains, $D = d_s = 1$, and tethered membranes, $D = d_s = 2$. The best-fitting exponents ν_0 and ν are shown in Table II. For *phantom* structures we used the corresponding Hausdorff dimensions d_0^H [see Eq. (2)] to estimate the spectral dimensions d_s of their backbone, see Eq. (3). The resulting estimates for d_s allow us to calculate Flory exponents ν_F according to Eq. (7). Numerical results are shown in Table II.

A. Phantom networks and d_s

The spectral dimension of Sierpinski gaskets can be obtained, for instance, by renormalization of vibrational modes [30] yielding

$$d_s^{\triangle} = 2 \ln 3 / \ln 5 = 1.365. \quad (9)$$

Using Eqs. (2), (5), and (9) it follows that $\nu_0 = 0.369$ for phantom SG structures. Our simulation results for ν_0 and the corresponding d_s approach their asymptotic expectations with increasing g, see Table II. This reproduces results from off-lattice Monte Carlo simulations [24] and supports the assumption of Gaussian elasticity.

By contrast, for phantom SCs we obtain higher values for ν_0, resulting in lower values for d_s as compared to previous results and predictions. In particular, our results for d_s remain below a lower bound that was given by Hattori *et al.* [43] applying a block-spin transformation on dual SCs. Watanabe

TABLE II. Simulation results for phantom and self-avoiding exponents ν_0 and ν, respectively, of polymeric fractals depending on generation, g. Results were obtained as best fits of the data shown in Fig. 4. In the case of obvious boundary effects we neglected linear sizes comparable to the whole structure for the fits. The spectral dimension d_s is extracted from ν_0 using Eqs. (5) and (2). The last column shows Flory result according to Eq. (7) using d_s of the same row. For Sierpinski gaskets we also display previous simulation results by Levinson [24]. We compare all simulation results to various exact and numerical predictions for d_s obtained by Rammal *et al.* [30], Hattori *et al.* [43], Reis [44], Barlow *et al.* [45], and Watanabe [46] with following ν_0 and ν_F according to Eqs. (5) and (7), respectively.

g	ν_0	d_s	ν	ν_F
		△ Sierpinski Gaskets		
7	0.382(13)	1.349(15)	0.763(7)	0.787(5)
8	0.382(7)	1.349(9)	0.765(16)	0.787(3)
9	0.379(11)	1.353(13)	0.752(46)	0.786(5)
Rammal *et al.*	0.369	1.365		0.781
Levinson	0.372(8)	1.361(9)	0.790(28)	0.783(3)
		□ Sierpinski Carpets		
4	0.225(2)	1.616(3)	0.911(9)	0.847(1)
5	0.199(4)	1.653(6)	0.957(13)	0.837(2)
6	0.180(5)	1.681(8)		0.829(2)
Hattori *et al.*	0.1534	1.721		0.819
Reis	0.104(11)	1.802(19)		0.799(14)
Barlow *et al.*	0.1021	1.80525		0.798
Watanabe	0.0701	1.862		0.785

[46] yielded an upper bound using a Migdal-Kadanoff bond-moving approximation. Probably the best estimates up to now have been found by Barlow *et al.* [45] and Reis [44]. They were obtained using numerical resistance calculations [45] and continuous SCs, as well as finite-size scaling of random walks [44] on dual SC lattices. The characteristics of SCs and their dual counterparts are expected to be identical for $g \to \infty$, but the convergence of d_s according to our simulations seems to be rather slow as compared to Ref. [45]. Besides boundary effects, this is due to the strong dependence of ramifications on g. The number of bonds connecting the largest subcarpets of a dual SC is $8 \times 3^{g-1}$ leading to an infinitely ramified structure for $g \to \infty$. On the other hand both dual and nondual SGs show a finite ramification, which is independent of generation. In terms of polymeric fractals, ramification should influence the number and distribution of elastically active strands and loops. To study the behavior of d_s for SCs in the limit $g \to \infty$ we plot simulation results against $1/g$ in Fig. 5. The available data points suggest a roughly linear convergence toward the expected limit $d_s^{\square} \approx 1.8$ [44,45] in this representation. Moreover, estimates for $d_s^{\square}$ using random walks on the carpet backbone according to Eq. (4) are comparable to our simulation results and show similar finite-size effects, see Fig. 5

In Fig. 6 we show our simulation results for d_s depending on the chemical dimension D compared to predictions using resistor analysis [45,47,48]. Here, predictions are also shown for various other generators, see Fig. 2, of the considered fractal classes. Figure 6 illustrates that if there exists some analytical expression $D(d_s)$ for one or more classes of regular

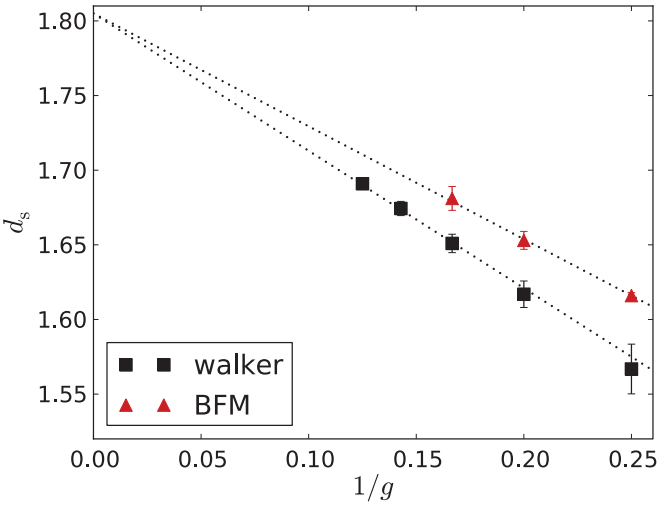

FIG. 5. (Color online) Estimates for the spectral dimension d_s of finite dual Sierpinski carpets as function of inverse generation. Here, we compare simulation results (▲) as given in Table II to statistics of random walks on SC lattices (■). The dotted lines are guides to the eye crossing each other at $d_s = 1.805$. The random walks used for this figure were carried out on SCs of various generations $4 \leqslant g \leqslant 8$ and with predefined number of sites to traverse, S_w. In particular, we defined $S_w^{(1)} = 64$ and $S_w^{(2)} = N/8$, where N is the total mass of the respective carpet. For a given pair (g, S_w) we created 10^4 walks and obtained the mean number of necessary steps, t. As an estimate for d_s we used the form $d_s \approx 2\log(S_w^{(2)}/S_w^{(1)})/\log(t_2/t_1)$, see Eq. (4).

planar fractals, it will not be universal for all generators. For instance, Fig. 6 shows an interpolation curve that is only valid for the SG family,

$$d_s(D) \approx 2 - \alpha(2 - D)^{\beta} \quad \text{with} \quad \alpha \approx 0.978, \quad \beta \approx 0.495, \tag{10}$$

where α and β are fitting parameters. We note, however, that our simulation result for $d_s^{\square}$ of Sierpinski carpets with generation $g = 6$ as shown in Fig. 6 is close to the interpolation curve (10) for the SG class due to finite-size effects as pointed out in Fig. 5. The interpolation (10) is consistent with an approximative form for $D \to 2$ discovered by Borjan *et al.* [47]. The nontrivial dependence of the spectral dimension of regular fractals on the characteristics of their generators such as ramification, death ends, or lacunarity have been discussed in the literature [50–52].

B. Excluded volume effects and ν

For self-avoiding Sierpinski gaskets the simulation results for ν as given in Table II are in agreement with the Flory exponent $\nu_F = 0.781$ according to Eqs. (7)–(9). This, again, confirms the results in Ref. [24]. Self-avoiding SGs in three-dimensional space are crumpled as expected.

Let us now focus on the simulation results for self-avoiding Sierpinski carpets as presented in Table II. Comparing the results for ν to Flory predictions ν_F based on simulation results for d_s and Eq. (7), it is obvious that there is an growing difference between ν and ν_F for increasing g. The disagreement between our results for ν and the prediction $\nu_F \approx 0.798$ based on the estimate $d_s^{\square} \approx 1.805$ [45] is even

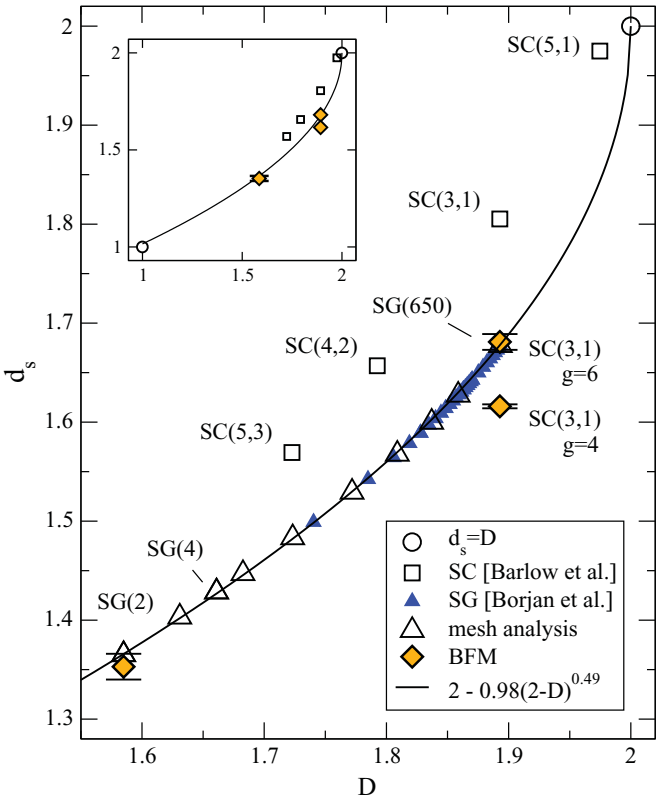

FIG. 6. (Color online) Spectral dimension d_s of polymeric Sierpinski gaskets and Sierpinski carpets (♦) obtained by BFM simulations according to Figs. 1(c) and 1(d). The graph shows data for SGs of generation $g = 9$ and for SCs of generations $g = 4$ as well as $g = 6$, see also Table II. Simulation results are compared to predictions based on resistance calculations for various symmetric generators (see Fig. 2) of the SC class (□, see Ref. [45]) and SG class (▲, see Ref. [47,48]). Furthermore, we applied a straightforward mesh analysis to calculate d_s for SG generators (△) based on Einstein relations [30,49]. For Sierpinski gaskets we found an empirical interpolation curve (continuous line), see Eq. (10). The inset gives an overview over the whole period $1 \leqslant D \leqslant 2$.

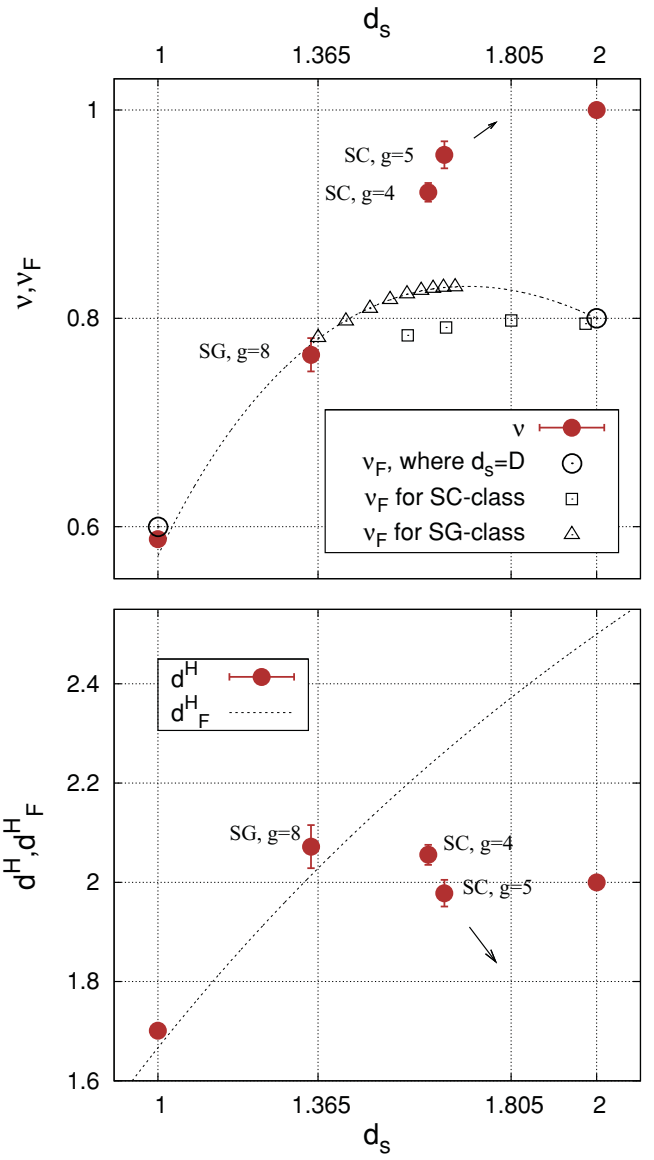

FIG. 7. (Color online) *Upper part:* Comparison between Flory predictions (△ and □), see Eq. (7), and simulation results (•) for ν according to Eq. (2) depending on the spectral dimension d_s. For fractal structures as illustrated in Fig. 1 we show data points (ν,d_s), where both ν and d_s are simulation results as given in Table II. For polymer chains ($d_s = 1$) and perfect membranes ($d_s = 2$) the well-known exponents $\nu = 0.588$ [23,32] and $\nu = 1$ [8] are displayed, respectively. The arrow indicates a possible asymptotic value for BFM-simulated Sierpinski carpets in the case $g \to \infty$. Flory predictions for fractals are obtained by setting theoretical and numerical results for d_s into Eq. (7). In particular for the Sierpinski gasket class (△) we applied mesh analyses for corresponding resistor networks to obtain d_s, see also Fig. 6 and Ref. [30]. The dotted line corresponds to an interpolation curve $d_s(D)$ found for SGs, see Eq. (10) and Fig. 6. Flory predictions for the SC class are based on estimates for d_s taken from Ref. [45]. *Lower part:* Comparison between Flory prediction d_F^H (dashed curve), see Eq. (7), and actual Hausdorff dimensions d^H (•) according to the data shown in the upper part and using Eq. (2).

larger. However, as the spectral dimension of the polymeric SCs used here lies below the latter estimate, we assume that the excluded volume effect should be less pronounced in those structures than in asymptotic carpets. Hence the deviation from the Flory result is even more notable.

From our simulation results it cannot be excluded that self-avoiding SCs are asymptotically flat for $g \to \infty$. This would imply the existence of a self-organized stiffening effect as it was argued also for self-avoiding tethered membranes [8], $d_s = 2$.

In Fig. 7 we compare Flory predictions ν_F and d_F^H to the actual exponents ν and d^H for polymer structures of various spectral dimension d_s. In the upper part of Fig. 7, ν_F is calculated using Eqs. (6) and (7) based on estimates for d_s, see Fig. 6 and Ref. [45]. For the exponents ν we show available simulation results for fractals, see Table II, as well as known values from the literature for polymer chains [23] and membranes [8]. While ν is close to ν_F for structures with lower values of d_s such as polymer chains and Sierpinski gaskets, one can see significant deviations both for Sierpinski

carpets and perfect membranes. As can be seen in Fig. 7, it is notable that the Flory prediction $\nu_F(d_s)$ for the SG class based on the interpolation curve, Eq. (10), implies a local maximum resulting from the interplay between d_s and D in Eq. (7). On the other hand, the available points $\nu_F(d_s)$ for the SC family do not imply such a maximum, see Fig. 7. As shown in the lower part of Fig. 7, the Flory-predicted Hausdorff dimension $d_F^H(d_s)$, see Eq. (7), is unique for all fractal families. Here, the relation $d_s \leftrightarrow D$ as pointed out in Fig. 6 is not involved, see Eq. (7). The simulation results for the Hausdorff dimensions of swollen networks, d^H, as shown in the lower part of Fig. 7 suggest that a hypothetical function $d^H(d_s)$ changes its monotonicity two times within the interval $1 \leqslant d_s \leqslant 2$. However, it would be more obvious that both d^H and ν depend not only on d_s but also on other features of the underlying generators such as ramification and loop structure. This has been questioned by Cates in Ref. [18].

C. Many-body contributions

Independently of the issue of entropic stiffness effects, which are not covered by the Flory free energy (6), one can check the self-consistency of result (7). In general all n-body interaction terms of the form [18]

$$c_n \left(\frac{N}{R^d}\right)^n R^d \propto c_n L^{Dn+\nu(1-n)d} \tag{11}$$

with coefficients c_n have to be considered in the free energy. Flory's result is self-consistent when 3-body and higher order contacts are not relevant for the solution. Repulsions of order n are relevant if $Dn + \nu(1-n)d > 0$ [21,54]. We can derive the following conditions using the Flory result, Eq. (7), in Eq. (11). The lowest order of self-contacts, n^*, which can be neglected is given by

$$n^*(d_s,d) = \frac{1 + d_s/2}{1 - d_s/d}. \tag{12}$$

Vice versa, if we require the negligence of order n, then the network connectivity has to fulfill

$$d_s \leqslant d_s^*(n,d) = \frac{n-1}{1/2 + n/d}. \tag{13}$$

Conditions (12) and (13) can be found analogously for integer values of d_s [21,54], where D replaces d_s. Although the replacement of D by d_s in Eqs. (12) and (13) seems to be a straightforward generalization for fractals, this result is in fact nontrivial (see also Fig. 6) and a particular consequence of the form of $d_0^H(d_s)$ in Eq. (5). Conditions (12) and (13) are presented graphically in Fig. 8. For Sierpinski gaskets in $d = 3$ one can observe that their spectral dimension $d_s^{\triangle} = 1.365$ is slightly above the threshold where 3-body repulsions become marginal, $d_s^*(3,3) = 4/3$, see Fig. 8. Within the Flory picture this suggests a small deviation toward $\nu > \nu_F$. Note that instead the Flory model can anyway produce a slight overestimate $\nu_F > \nu$ as is the case for polymer chains in $d = 3$. However, possible deviation in any direction has not been detected up to now, see Table II and Ref. [24].

Note also that for SGs in two dimensions one would have to regard terms up to order $n^*(d_s^{\triangle},2) \approx 5.30$ which is comparable

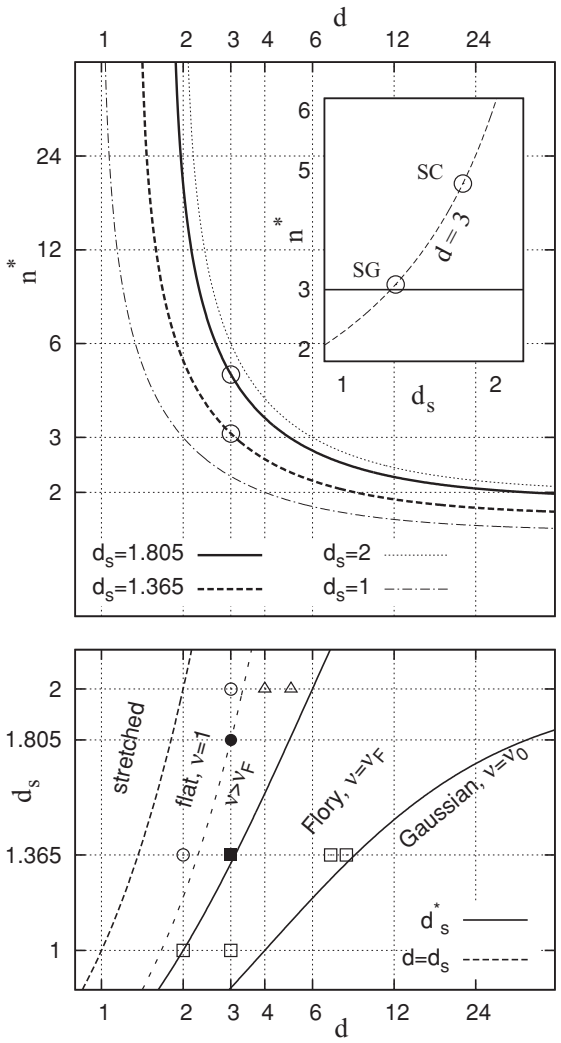

FIG. 8. *Upper part:* Lowest order n^* of self-contact energies [see Eq. (11)] that can be neglected in terms of the Flory ansatz Eq. (6). We show n^* as function of space dimension d for various polymer architectures with spectral dimension d_s, see Eq. (12). Open circles mark polymeric fractals as treated in this work. The inset is a cut through the $n^*(d_s,d)$ surface at space dimension $d = 3$. *Lower part:* Hypothetical phase diagram. Solid lines show spectral dimension $d_s^*(d,n = 2)$ (lower curve) and $d_s^*(d,n = 3)$ (upper curve) where n-point terms can be neglected within the Flory picture, see Eq. (13). The lower solid curve illustrates the upper critical space dimension, whereas the dashed curve marks the lower critical dimension $d = d_s$ [18]. The sparsely dashed curve is a hypothetical boundary between stronger swelling $\nu > \nu_F$ due to higher order contributions in Eq. (6) and a flat phase ($\nu = 1$) due to self-organized bending stiffness. Closed symbols show points that are treated in our computer simulations, see Table II. Circles mark points where computer simulations yield a flat phase, in particular as indicated for $(2,d_s^{\triangle})$ [25] and $(3,d_s^{\square})$ (see Table II) as well as proven for (3,2) [8]. Squares represent swollen structures where deviations between Flory exponents and numerical results are much smaller as compared to SCs (see Table II) or not detected up to now, in particular (2,1) [53], (3,1) [23], $(3,d_s^{\triangle})$ (see [24] and Table II), and SGs in 7 and 8 dimensions [24]. Monte Carlo simulations of tethered membranes ($d_s = 2$) in 4 and 5 dimensions ($\triangle$, see Ref. [5]) yield $\nu > \nu_F$. Compare also to Fig. 5 in Ref. [24].

magnitude to $n^*(2,3) = 6$, see also the upper part of Fig. 8. This may correspond to the stretched behavior, $\nu = 1$, concluded in Ref. [25].

In the lower part of Fig. 8 we consider a phase diagram following Levinson [24] to graphically represent the various states of fractal membranes. Here, it is completed by data for self-avoiding Sierpinski carpets. The Flory prediction for SCs in $d = 3$ is not self-consistent as $d_s^{\square} \approx 1.805$ [45] is significantly larger than $d_s^*(3,3) = 4/3$. At least 4-point terms would have to be considered in a self-consistent model, since $n^*(d_s^{\square},3) \approx 4.78$. This indicates the dominance of excluded volume interactions in the structures' elasticity and supports the results in Table II which suggest asymptotically flat SCs in $d = 3$. However, the universality of this conclusion has to be checked, for instance by tests with different simulation methods.

V. CONCLUSIONS

The embedding of planar polymeric fractals into three-dimensional space has been studied using Monte Carlo simulations. In particular we considered Sierpinski gaskets and Sierpinski carpets of various generations. By simulation of phantom structures we estimated the spectral dimensions d_s of fractal backbones assuming Gaussian elasticity. We have shown that for increasing generation the resulting estimates for d_s of both SGs and SCs are converging toward theoretical and numerical predictions for infinite fractals. However, SCs show a much slower convergence as compared to SGs. This should be a consequence of qualitative differences between the fractals such as ramification or hole structure and particularly their dependencies on generation. We conclude that polymeric fractals without excluded volume can be described by Gaussian elasticity depending on their spectral dimension only, but finite-size effects may depend also on other characteristics provided by the generator class.

Self-avoiding polymeric fractals in athermal solvent have been simulated to compare a generalized Flory argument to the actual swelling effects. Our simulation results confirm that SGs are crumpled and the corresponding Flory prediction is within the error bars. For SCs, on the other hand, we see a proven discrepancy between Flory exponents and simulation results. Furthermore our results suggest that Sierpinski carpets are not crumpled, but asymptotically flat comparable to tethered membranes. This indicates the presence of self-organized bending stiffness in Sierpinski carpets, that is, for spectral dimensions $d_s < 2$. We note that in contrast to phantom polymeric fractals, both the fixed points of swollen polymeric fractals as well as their finite-size effects may depend on more features of the underlying generators than d_s only.

Following Levinson [24] we considered a phase diagram based on our simulation results and discussions. The diagram shows the conformational states of regular fractals as a function of external space dimension and spectral dimension. Based on a test for the self-consistency of the Flory prediction regarding the scaling of higher order contributions in a virial expansion we discussed the location of various polymeric fractals within this diagram. For Sierpinski gaskets there is only a marginal inconsistency in three space dimensions which suggests a slightly stronger swelling than predicted by the Flory argument. In fact, the spectral dimension of SGs is very close to the limiting value of $d_s = 4/3$, below which Flory arguments based on a second virial coefficient are self-consistent. Thus, SGs should be located in a crossover region between higher spectral dimensions, where swelling is stronger than predicted by the Flory model, and smaller spectral dimensions, where Flory predictions are self-consistent.

For Sierpinski carpets one can show that the Flory prediction is not self-consistent. Here, we obtain a lower value of 4-body interactions which have to be taken into account. Involving also our simulation results as discussed above, we locate SCs near the boundary between the region of stronger swelling due to higher order contributions and even larger values of the spectral dimension (but smaller than space dimension) where stretched structure cannot be excluded, at least on sufficiently large finite sizes. The impact of higher order virial coefficients on the effect of self-organized stiffness as well as the exact form of the corresponding phase diagram are open issues.

The tendency of fractal structures with spectral dimensions closer to 2D to display quasistretched behavior indicates a certain robustness of this feature for membranes with respect to defects in their connectivity.

[1] J. H. Fendler and P. Tundo, Acc. Chem. Res. **17**, 3 (1984).
[2] J. H. Fendler, Chem. Rev. **87**, 877 (1987).
[3] T. Hwa, E. Kokufuta, and T. Tanaka, Phys. Rev. A **44**, R2235 (1991).
[4] M. Plischke and D. Boal, Phys. Rev. A **38**, 4943 (1988).
[5] D. Boal, E. Levinson, D. Liu, and M. Plischke, Phys. Rev. A **40**, 3292 (1989).
[6] F. F. Abraham, W. E. Rudge, and M. Plischke, Phys. Rev. Lett. **62**, 1757 (1989).
[7] J.-S. Ho and A. Baumgärtner, Phys. Rev. Lett. **63**, 1324 (1989).
[8] Y. Kantor and K. Kremer, Phys. Rev. E **48**, 2490 (1993).
[9] M. Werner, Diploma thesis, Technische Universität Dresden and Leibniz Institut für Polymerforschung Dresden, 2009.
[10] M. J. Bowick and A. Travesset, Phys. Rep. **344**, 255 (2001).
[11] F. F. Abraham and D. R. Nelson, J. Phys. (France) **51**, 2653 (1990).
[12] D. R. Nelson and L. Peliti, J. Phys. (France) **48**, 1085 (1987).
[13] J. A. Aronovitz and T. C. Lubensky, Phys. Rev. Lett. **60**, 2634 (1988).
[14] P. Le Doussal and L. Radzihovsky, Phys. Rev. Lett. **69**, 1209 (1992).
[15] Y. Kantor and D. R. Nelson, Phys. Rev. Lett. **58**, 2774 (1987).
[16] M. Baig, D. Espriu, and A. Travesset, Nucl. Phys. B **426**, 575 (1994).
[17] M. Baig, D. Espriu, and J. F. Wheater, Nucl. Phys. B **314**, 587 (1989).
[18] M. E. Cates, Phys. Rev. Lett. **53**, 926 (1984).

[19] Y. Kantor, M. Kardar, and D. R. Nelson, Phys. Rev. Lett. **57**, 791 (1986).
[20] Y. Kantor, M. Kardar, and D. R. Nelson, Phys. Rev. A **35**, 3056 (1987).
[21] T. Hwa, Phys. Rev. A **41**, 1751 (1990).
[22] F. David and K. J. Wiese, Phys. Rev. Lett. **76**, 4564 (1996).
[23] N. Clisby, R. Liang, and G. Slade, J. Phys. A **40**, 10973 (2007).
[24] E. Levinson, Phys. Rev. A **43**, 5233 (1991).
[25] E. Duering and Y. Kantor, Phys. Rev. B **40**, 7443 (1989).
[26] Y. Kantor, Physica D **38**, 215 (1989).
[27] J.-U. Sommer and A. Blumen, J. Phys. A **28**, 6669 (1995).
[28] D. Nelson, T. Piran, and S. Weinberg, *Statistical Mechanics of Membranes and Surfaces* (World Scientific, Singapore, 1989), p. 115.
[29] S. Alexander and R. Orbach, J. Phys. Lett. **43**, L625 (1982).
[30] R. Rammal and G. Toulouse, J. Phys. Lett. **44**, L13 (1983).
[31] S. Havlin and D. Ben-Avraham, Adv. Phys. **36**, 695 (1987).
[32] P.-G. de Gennes, *Scaling Concepts in Polymer Physics* (Cornell University Press, New York, 1991).
[33] L. P. Kadanoff, Ann. Phys. **100**, 359 (1976).
[34] A. Billoire, D. J. Gross, and E. Marinari, Phys. Lett. B **139**, 75 (1984).
[35] H. P. Deutsch and K. Binder, J. Chem. Phys. **94**, 2294 (1991).
[36] I. Carmesin and K. Kremer, Macromolecules **21**, 2819 (1988).
[37] C. Hagn, M. Wittkop, S. Kreitmeier, H. L. Trautenberg, T. Hölzl, and D. Göritz, Polymer Gels and Networks **5**, 327 (1997).
[38] J.-U. Sommer, M. Schulz, and H. L. Trautenberg, J. Chem. Phys. **98**, 7515 (1993).
[39] J.-U. Sommer, T. A. Vilgis, and G. Heinrich, J. Chem. Phys. **100**, 9181 (1994).
[40] S. Lay, J.-U. Sommer, and A. Blumen, J. Chem. Phys. **113**, 11355 (2000).
[41] H. L. Trautenberg, T. Hölzl, and D. Göritz, Comput. Theor. Polym. Sci. **6**, 135 (1996).
[42] B. B. Mandelbrot, *The Fractal Geometry of Nature* (Freeman, San Francisco, 1982).
[43] K. Hattori, T. Hattori, and H. Watanabe, Phys. Rev. A **32**, 3730 (1985).
[44] F. D. A. A. Reis, J. Phys. A **28**, 6277 (1995).
[45] M. T. Barlow, R. F. Bass, and J. D. Sherwood, J. Phys. A **23**, L253 (1990).
[46] H. Watanabe, J. Phys. A **18**, 2807 (1985).
[47] Z. Borjan, S. Elezović, M. Knežević, and S. Milošević, J. Phys. A **20**, L715 (1987).
[48] S. Milošević, D. Stassinopoulos, and H. E. Stanley, J. Phys. A **21**, 1477 (1988).
[49] J. A. Given and B. B. Mandelbrot, J. Phys. A **16**, L565 (1983).
[50] R. Dasgupta, T. K. Ballabh, and S. Tarafdar, J. Phys. A **32**, 6503 (1999).
[51] F. D. A. A. Reis, J. Phys. A **29**, 7803 (1996).
[52] M. H. Kim, D. H. Yoon, and I. Kim, J. Phys. A **26**, 5655 (1993).
[53] B. Derrida, J. Phys. A **14**, L5 (1981).
[54] G. Gompper and D. M. Kroll, J. Phys. Condens. Matter **9**, 8795 (1997).